JOURNAL OF GUIDANCE, CONTROL, AND DYNAMICS
Vol. 30, No. 2, March–April 2007

Further Results on the Controllability of a Two-Wheeled Satellite

Frédéric Boyer*
Ecole des Mines de Nantes, 44000 Nantes, France
and
Mazen Alamir†
Laboratoire d'Automatique de Grenoble, 38400 St. Martin d'Hères, France

DOI: 10.2514/1.21505

This article deals with the open-loop attitude control of a satellite actuated by two reaction wheels when the kinetic momentum is not necessarily equal to zero. Hence this article helps to answer the following question: "What is the most to be expected in such conditions?" As a matter of fact, the satellite with two reaction wheels and non-null kinetic momentum is not controllable over the entire state space of the spacecraft attitudes. Nevertheless, a five-dimensional subspace of feasible states is potentially reachable. In this article, this subset will be explicitly defined and the reachability of two control objectives related to it will be studied. The first objective deals with steering the satellite from any feasible attitude state to any feasible rest state. The second deals with steering the spacecraft from any feasible state to any given configuration irrespective of the spin about the nonactuated spacecraft axis. This article gives constructive demonstrations of reachability rather than qualitative answers, because it presents open-loop control laws based on path planning compatible with these two objectives. Finally, some simulation results illustrate the feasibility of the approach.

I. Introduction

TECHNOLOGICALLY, satellite attitude is mostly controlled by momentum exchange devices or gas jet thrusters. In spite of their apparent similarities, the problems of control raised by these two types of technology are drastically different. In the first case, the satellite changes its attitude by inertial transfers via a momentum conservation law as in the case of a "falling cat" [1], whereas in the second it moves thanks to reaction forces generating genuine external torques. Whatever the type of actuator, the first studies on attitude control in the case of actuator failures dealt with questions of controllability and were by Bonnard [2] and Crouch [3]. In particular, the second author showed that in the case of a satellite actuated with momentum wheels, controllability fails when there are fewer than three actuators. This is probably why the control community primarily investigated the case of spacecraft underactuated with gas jets [4–6].

In this paper, we focus our attention on the open-loop attitude control of a satellite actuated with two inertia wheels and try to answer the following question [7]: "What is the most one can expect in such a case?" In this case, the satellite is generally not controllable, however, any attitude remains reachable at rest when the satellite total momentum is zero. Thus, most of the solutions proposed today for controlling satellites with two rotors deal with stabilization in this restricted case. Moreover, because the dynamics do not respect Brockett's condition, these solutions are time varying feedbacks or nonsmooth ones [8,9]. Other studies [10] deal with the more general case where the kinetic momentum is not zero but consider the stabilization problem of the unactuated axis irrespective of the rotation state around itself. In this restricted context, the state space is four dimensional and it is possible to design some smooth static feedback laws. Here we consider the general case of attitude control with a non-null kinetic momentum and include rotation about the unactuated axis in the control objectives. We shall prove that the failure of a rotor imposes a nonholonomic constraint forcing the feasible spacecraft state space to be a five-dimensional subset of the attitudes' state space. This constraint will be used to define two types of objective compatible with it, while being relevant to practical applications. Thus control is designed on the maximal five-dimensional space of the feasible states. In the first objective, the final velocity is imposed to be zero, whereas in the second, it is the final attitude that is arbitrarily fixed, irrespective of the value of the angular velocity about the nonactuated axis. Hence, the attitude reaches the desired attitude at the final time and follows its motion with its own angular velocity. Moreover, we shall prove that these two objectives are reachable from any state of the feasible state space.

This article proposes an explicit constructive procedure for deriving open-loop steering laws rather than giving qualitative results to the reachability problem. This procedure is based on the definition of two variables whose time evolution allows us to reconstruct all the state variables and finally the control torques. Note here that in spite of some similarities, these variables are not "flat outputs" [11] because the reconstruction process is not only based on algebraic relations but also on integral ones. Moreover, the proposed solution is intimately based on the geometry of the unit sphere S^2, revealing the role of its curvature in the control and exhibiting some "geometric phases" and "dynamic phases," as in the "falling cat problem" [1]. Finally, the open-loop control proposed here will be used in the future to achieve nonsmooth feedback laws based on a receding horizon strategy [12].

The paper is structured as follows. First, following previous studies [13–15] on the control problem of a one-axis underactuated spacecraft, its attitude space SO(3) will be identified to $S^2 \times \mathrm{SO}(2)$ (Sec. II). The open-loop control strategy will be presented in Sec. III. In Sec. IV, this control law is associated with a path-planning algorithm derived from the stereographic chart of S^2 introduced by Tsiotras and Longuski [14] and first restricted to one of its open subsets (Sec. V). Finally, Sec. VI deals with singularities and extends the reachability of the two objectives to the whole feasible space. Before concluding (Sec. VIII) some simulation results are given in Sec. VII in the simplest and most pathological cases.

Received 1 December 2005; revision received 3 March 2006; accepted for publication 4 March 2006.

*Assistant Professor, Institut de Recherche en Communication et Cybernétique de Nantes, 1 Rue de La Noë.

†Chargé de Recherche Centre National de la Recherche Scientifique, BP 46, Domaine Universitaire.

II. Modeling

A. Basic Definitions and Notations

We will consider a satellite with two-inertia wheels (rotors) as displayed in Fig. 1. Applying standard parametrization of the rigid body to the satellite, we introduce a fixed inertial frame (O, e_1, e_2, e_3) and a mobile frame attached to the satellite's body (O, t_1, t_2, t_3). These two frames are related by

$$t_i = Re_i, \qquad i = 1, 2, 3 \tag{1}$$

where $R \in \mathrm{SO}(3)$, and the e_i's are identified to the canonical basis of $\mathbb{R}^3$. The vector of angles $q = (q_1, q_2)^T \in \mathbb{R}^2$, will parametrize the rotor dynamics. Throughout this article, $\hat{V}$ is the skew-symmetric 3-3 matrix paired to any $V \in \mathbb{R}^3$, while $(\hat{V})^\vee = V$. Finally, $\mathrm{rot}(x, \theta)$, $\mathrm{rot}(y, \theta)$, and $\mathrm{rot}(z, \theta)$ will denote the three planar rotations of an angle θ about the three axes x, y, and z respectively.

B. Geometric Modeling of the Problem

Because one of the three mobile axes (here t_3) is distinguished by its nonactuated character, it is relevant to parametrize SO(3) as follows:

$$R = \mathrm{rot}(z, \lambda)\Lambda(t_3) \tag{2}$$

where $\Lambda(t_3) \in \mathrm{SO}(3)$ is any rotation such that $\Lambda(t_3)e_3 = t_3$. Because e_3 and t_3 are two-unit vectors, we can identify them to two points of the unit sphere S^2. Hence, any $\Lambda(t_3)$ is naturally parametrized by two coordinates on the unit sphere. For instance, adopting the following parametrization of $\Lambda(t_3)$:

$$\Lambda(t_3) = \mathrm{rot}(x, \psi)\mathrm{rot}(z, \varphi) \tag{3}$$

corresponds to parametrizing the unit sphere by two spherical coordinates where φ is the longitude and ψ is the latitude on the open set $S^2 - \{\pm e_3\}$, where $+e_3$ and $-e_3$ stand for the north and south poles of S^2, respectively. Moreover, in this case:

$$t_3 = Re_3 = \Lambda(t_3)e_3 = \begin{pmatrix} \sin\varphi \sin\psi \\ -\cos\varphi \sin\psi \\ \cos\psi \end{pmatrix} \tag{4}$$

Finally, (2) defines a parametrization of any $R \in \mathrm{SO}(3) - \{R/R(\pm e_3) = \pm e_3\}$, where $R(\pm e_3) = \pm e_3$ means $Re_3 = e_3$ and $R(-e_3) = -e_3$. This convention is systematically used in the article. Next, we shall use the following notations for the subsets of the unit sphere and the group of rotations introduced above:

$$\begin{aligned} \mathcal{U} &\triangleq (S^2 - \{\pm e_3\}) \subset S^2 \\ \mathcal{W}_\pm &\triangleq \{R \in \mathrm{SO}(3)/R(\pm e_3) = \pm e_3\} \subset \mathrm{SO}(3) \\ \mathcal{V} &\triangleq \{\mathrm{SO}(3) - \mathcal{W}_\pm\} \subset \mathrm{SO}(3) \end{aligned} \tag{5}$$

Finally, combining (2) and (3) shows that (φ, ψ, λ) are the three Euler's angles of a $3-1-3$ sequence on $\mathcal{V} \subset \mathrm{SO}(3)$. Hence, the two polar singularities of S^2 stand for those of any "three-angle" parametrization of SO(3). For instance, in Sec. VI, the unit sphere will be coordinatized with a stereographic projection defined on $\mathcal{U} = S^2 - \{\pm e_3\}$.

Remark: It is worth noting that even if the adopted parametrization is an Euler's sequence well adapted to our problem, geometrically this parametrization splits the spacecraft attitude $R \in \mathrm{SO}(3)$ into that of $t_3 \in S^2$, plus the rotation about t_3 parametrized by a single angle λ. Hence, $\mathrm{SO}(3) \cong S^2 \times \mathrm{SO}(2)$ is a "principal fiber bundle" with S^2 the base manifold, and SO(2) the structure group (named the "fiber"). This structure is crucial because it allows us to define a natural way of relating the motion of the nonactuated axis to the rotation around it. This relation will now be explained. It is based on the concept of connection on a fiber bundle.

C. Kinematic Model

Because $\mathrm{SO}(3) \cong S^2 \times \mathrm{SO}(2)$, we now have to link the satellite kinematics on these two definitions of its configuration space. This is the purpose of the following.

1. *Kinematics on* SO(3)

The kinematics on SO(3) is defined by

$$\Omega = (R^T\dot{R})^\vee \tag{6a}$$

$$\omega = (\dot{R}R^T)^\vee \tag{6b}$$

where $\Omega \in \mathrm{SO}(3)$ [respectively, $\omega \in \mathrm{SO}(3)$] is the angular velocity of the spacecraft in the body frame (respectively, in the inertial frame).

2. *Kinematics of the Nonactuated Axis (on S^2)*

It is simply expressed in $\mathbb{R}^3$ by

$$\dot{t}_3 = \omega \times t_3 = \Omega_2 t_1 - \Omega_1 t_2 = \left(t_1^T\dot{t}_3\right)t_1 + \left(t_2^T\dot{t}_3\right)t_2 \tag{7}$$

or directly in the spherical coordinates by time differentiating (4). Furthermore, as a point of $\mathbb{R}^2$, the velocity of t_3 is simply expressed in the spherical chart by $\dot{t}_3 = \dot{\varphi}\partial_\varphi + \dot{\psi}\partial_\psi$ [with $(\partial_\varphi, \partial_\psi)$ the natural basis of the chart].

3. *Kinematics of the Rotation About the Nonactuated Axis [in the Fiber* SO(2)*]*

Inserting (2) into (6a) and keeping the third row of the result, we find

$$\dot{\lambda} = \Omega_3 - (\cos\psi)\dot{\varphi} \tag{8}$$

At this point, let us note that whereas (as we shall see later) Ω_3 in (8) is ruled by the dynamics of the spacecraft, the second term "$-(\cos\psi)\dot{\varphi}$" is only related to the intrinsic geometry of S^2. Indeed, this second term is the expression in spherical coordinates of the "Levi–Civita connection one form on S^2" that we note ω_{S^2}. This type of object is a linear form mapping vectors onto scalars (here the velocities $\dot{\lambda}$). In fact, it can be proved that the Levi–Civita connection one form of the sphere is defined in the spherical chart by

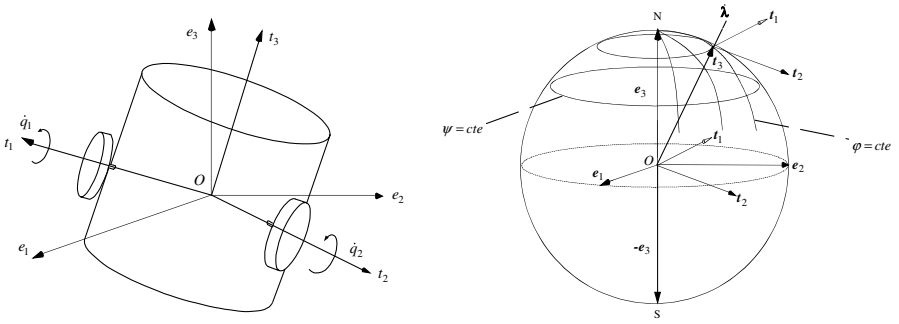

Fig. 1 Satellite with two rotors, and attitude parametrization.

$\omega_{S^2} = -(\cos\psi)\,\mathrm{d}\varphi$. Hence, when acting on any vector tangent to S^2, like the velocity of the nonactuated axis tip as a point of $\mathbb{R}^2$, that is $\dot{t}_3 = \dot{\varphi}\partial_\varphi + \dot{\psi}\partial_\psi$, we have

$$\omega_{S^2}(\dot{t}_3) = -(\cos\psi)\,\mathrm{d}\varphi(\dot{\varphi}\partial_\varphi + \dot{\psi}\partial_\psi) = -\cos\psi[\dot{\varphi}\,\mathrm{d}\varphi(\partial_\varphi) + \dot{\psi}\,\mathrm{d}\varphi(\partial_\psi)] = -\cos\psi\dot{\varphi}1 + 0 = -\cos\psi\dot{\varphi}$$

Finally, (8) can be rewritten intrinsically (without any coordinates on the sphere) as

$$\dot{\lambda} = \Omega_3 + \omega_{S^2}(\dot{t}_3) \tag{9}$$

Hence, when $\Omega_3 = 0$ everywhere on S^2 (i.e., as we shall see later, when the kinetic momentum of the spacecraft is zero), (9) reduces to $\dot{\lambda} = \omega_{S^2}(\dot{t}_3)$. Then, $\dot{\lambda}$ geometrically represents the angular velocity about t_3 applied to the mobile frame (t_1, t_2) tangent to S^2 while being parallel transported along $\dot{t}_3$ on S^2 (with t_3 driven by the two actuated rotors). Moreover, this rotating motion is produced by any deviation of the trajectory of t_3 on the unit sphere with respect to its great circles. This is shown by remarking that $\cos\psi d\varphi(\dot{t}_3) = 0$ along any path: $t \in \mathbb{R} \mapsto t_3(t) \in S^2$, such that $\psi(t) = \pi/2$ or $\varphi(t) = cte$. This context is summarized in Fig. 2 between two instants t_o and t, where $[t_{1,\parallel}(t_o), t_{2,\parallel}(t_o)]$ is the parallel transport of the frame $[t_1(t_o), t_2(t_o)]$ along the great circle linking $t_3(t_o)$ and $t_3(t)$. Finally, when the kinetic momentum of the spacecraft is zero and so: $\Omega_3 = 0$ everywhere on S^2, it is thanks to this property of S^2 (as a Riemannian space with non-null curvature) that the failure of one control can be compensated by the two others.

On the other hand, we shall see later that the simple geometric context above is not sufficient in the case where the kinetic momentum is non-null. In fact, in this more general case, path planning requires invoking the dynamics of the satellite as below.

D. Dynamic Modeling

From standard Euler theorems applied to the satellite's configuration space: $\mathrm{SO}(3) \times \mathbb{R}^2$, the satellite dynamics can be written in the inertial frame as

$$d(I\omega + \tilde{I}_r\dot{q})/\mathrm{d}t = 0 \tag{10a}$$

$$d\left(\tilde{I}_r^T\omega + \bar{J}_r\dot{q}\right)/\mathrm{d}t = \tau \tag{10b}$$

with $\tau = (\tau_1, \tau_2)^T$ the control torque vector, and the following inertia tensors $I = RJR^T$, $\tilde{I}_r = R\tilde{J}_r$, $J = J_s + J_r$, with $J_s = \mathrm{diag}_{i=1,2,3}(J_{si})$, $J_r = \mathrm{diag}_{i=1,2,3}(J_{ri})$, $\bar{J}_r = \mathrm{diag}_{\alpha=1,2}(J_{r\alpha})$ and $\tilde{J}_r$ is deduced from $\bar{J}_r$ by adding to it, a third null 1×2 row. The J_{si}'s are the principal inertia moments of the satellite (with its rotors), and the J_{ri}'s are those of the rotors around their own axis ($J_{r3} = 0$). Moreover, introducing the total kinetic angular momentum in the inertial and body frames

$$\sigma = I\omega + \tilde{I}_r\dot{q} \tag{11a}$$

$$p = R^T\sigma = J\Omega + \tilde{J}_r\dot{q} \tag{11b}$$

allows rewriting (10a) as the conservation law:

$$\sigma = \sigma(t_o) = \sigma_o \tag{12}$$

whereas in the mobile frame, (10) can be rewritten as

$$\dot{p} + \Omega \times p = 0, \tag{13a}$$

$$\tilde{J}_r^T\dot{\Omega} + \bar{J}_r\ddot{q} = \tau \tag{13b}$$

In the following, (11–13) are used to design the open-loop control.

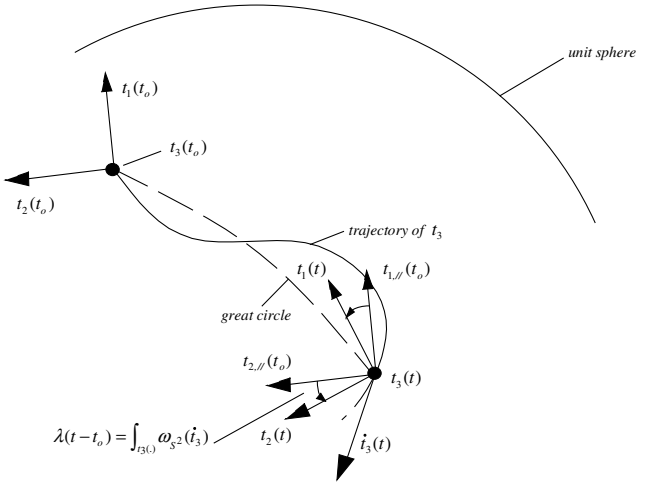

Fig. 2 Role of the curvature (connection) when kinetic momentum is zero.

III. Open-Loop Control Design

Next, we shall use the following notations: $T\mathrm{SO}(3)$ is the state space of orientation velocities of the satellite, that is $T\mathrm{SO}(3) \triangleq \{x = (R, \Omega) \in \mathrm{SO}(3) \times \mathrm{SO}(3)\}$. Moreover, with the parametrization (2), $T\mathrm{SO}(3)$ can be identified to $TS^2 \times T\mathrm{SO}(2)$, where $TS^2 \triangleq \{(t_3, \dot{t}_3)/t_3^T t_3 = 1, t_3^T\dot{t}_3 = 0\}$, and $T\mathrm{SO}(2) \triangleq \{(\lambda, \dot{\lambda}) \in \mathbb{R}^2\}$. This extension from configuration space to state space leads us to introduce the following sets of states associated with the configuration sets of (5), that is

$$T\mathcal{U} \triangleq \{(t_3, \dot{t}_3)TS^2/t_3 \neq \pm e_3\}$$

$$T\mathcal{W}_\pm \triangleq \{(R, \Omega)T\mathrm{SO}(3), \text{ with } R/R(\pm e_3) = \pm e_3\}$$

$$T\mathcal{V} \triangleq T\mathrm{SO}(3) - T\mathcal{W}_\pm$$

We will first define the feasible state space of the spacecraft attitude, that is, the subspace of $x = (R, \Omega) \in T\mathrm{SO}(3)$ compatible with the dynamics (11–13).

A. Feasible Space

Because of the symmetry of the system with respect to the axe of poles, we place (O, e_1, e_2, e_3) such that $e_3 \sim \sigma_o$, that is

$$\sigma_o = \left(e_3^T\sigma_o\right)e_3 = \sigma_{o3}e_3 \tag{14}$$

Assertion 1: With (14), and $A = \sigma_{o3}/J_3$, the feasible state space $\mathcal{A}$ of the spacecraft attitude is a five-dimensional subspace defined by

$$\mathcal{A} \triangleq \left\{x = (R, \Omega) \in T\mathrm{SO}(3)/\Omega_3 = \mathcal{A}\left[e_3^T(Re_3)\right]\right\} \tag{15}$$

Proof: First, equalize (11b) with $R^T\sigma_o$ and then project the result onto e_3. Then (14) defines the following constraint on $T\mathrm{SO}(3)$:

$$\Omega_3 = A\left[e_3^T(Re_3)\right] = A\left(e_3^Tt_3\right) \tag{16}$$

whose kernel is a nonintegrable level set of $T\mathrm{SO}(3)$ because Ω_3 is not the time derivative of any generalized attitude coordinate. Thus, (16) represents a constraint to the motion irrespective of the controls applied [3]. This explains why the satellite dynamics cannot be generally reachable and therefore not controllable on $T\mathrm{SO}(3)$. □

Finally, (16) shows that when $\sigma_o \neq 0$, then Ω_3 is not equal to zero on the whole sphere. Hence, the kinematics depicted in Fig. 2 are not sufficient for path planning. All the subsequent developments deal with this more general case.

B. Control Objectives

We are now going to consider two control objectives both relevant to applications and feasible, that is, compatible with (16). The first one (O1) consists in steering the satellite to a rest position. The second objective (O2) consists in steering the satellite to a given attitude, irrespective of the value of the angular velocity about the nonactuated axis. Moreover, in the two cases, the orientation λ about t_3 is included in the target objective. Hence the two control objectives are defined on the maximal feasible state space. Based on these two objectives, we are going to define two sets of feasible states which verify them. Then in Secs. III and IV we will introduce the open-loop control strategy and the path-planning algorithm on which the next two sections (V and VI) are based and which deal with reachability.

Objective 1: O1 We will first focus our interest on feasible target states x with spacecraft attitude at rest. This objective is particularly relevant with respect to practical aiming applications. It is defined by the space of feasible states at rest:

$$(\mathcal{A}_1 \subset \mathcal{A}) \triangleq \Big\{ x = (R, \Omega) T\mathrm{SO}(3), \text{ with } R/A\Big[e_3^T(Re_3)\Big] = 0 \text{ and } \Omega/\Omega_1 = \Omega_2 = 0 \Big\} \tag{17}$$

Note that when $A = 0$ (i.e., $\sigma_o = 0$), all the attitudes are feasible at rest. On the other hand, when $\sigma_o \neq 0$, (16) imposes any feasible attitude at rest to be such that σ_o is contained in the plane of the two wheels. This is the condition necessary to transfer the kinetic momentum from the satellite's attitude dynamics to those of the wheels.

Objective 2: O2 Alternatively, it may be interesting to steer the spacecraft from any feasible state to a state with an arbitrary desired final orientation $R \in \mathrm{SO}(3)$ irrespective of the velocity about t_3. In such a case, with $\Omega_\alpha = 0$ ($\alpha = 1, 2$), (16) forces the satellite to spin around its nonactuated axis with the velocity $\Omega_3 = A(e_3^T t_3)$. This second set of objectives defines the space of feasible states with a specified orientation R:

$$(\mathcal{A}_2 \subset \mathcal{A}) \triangleq \Big\{ x = (R, \Omega) T\mathrm{SO}(3)/R \in \mathrm{SO}(3) \text{ and } \Omega_\alpha = 0, \Omega_3 = A\Big[e_3^T(Re_3)\Big] \Big\} \tag{18}$$

In the following, we shall denote by $\mathcal{A}^\circ$ and $\mathcal{A}_2{}^\circ$, respectively, the $\mathcal{A}$ and $\mathcal{A}_2$ spaces without $T\mathcal{W}_\pm$. Note that this restriction does not concern $\mathcal{A}_1$. As far as O1 is concerned, we have two cases: 1°) If $\sigma_o = 0$, then the frame (O, e_1, e_2, e_3) can be placed anywhere to circumvent the charts' singularities of S^2. 2°) If $\sigma_o \neq 0$, (16) necessarily imposes any state of $\mathcal{A}_1$ to verify $t_3 \neq \pm e_3$. Finally, let us note that if $A = 0$ then $\mathcal{A}_1 = \mathcal{A}_2$, whereas in all cases: $\mathcal{A}_1, \mathcal{A}_2{}^\circ \subset \mathcal{A}^\circ$.

C. Open-Loop Control Strategy

Based on these two objectives (O1, O2) the following open-loop control problem arises. Let us consider any initial state $x_o \in \mathcal{A}$, and desired final state: $x_f \in \mathcal{A}_1$ or $\mathcal{A}_2$. Then, find a torque law $\tau(.)$: $t \in [t_o, t_f] \mapsto \tau(t)$ that steers x from x_o to x_f. Thus, if such a law can always be found, $\mathcal{A}_1$ and $\mathcal{A}_2$ will be considered as reachable from $\mathcal{A}$ in a finite time $t_f - t_o$. Moreover, if such an open-loop control exists on an infinite time interval, that is, $\tau(.)$: $t \in [t_o, +\infty[\mapsto \tau(t)$ exists, such that $x(t_o) = x_o$, and $x(+\infty) = x_f$, then $\mathcal{A}_1$ and $\mathcal{A}_2$ will be considered as "asymptotically reachable" from $\mathcal{A}$. In the following, we will consider first the open-loop control problem in finite time even though (see remark 2 of Sec. IV), the control will later be designed on an infinite time interval. The proposed solution to this control problem is based on the path-planning strategy proposed in the next section and on the following "assertion."

Assertion 2: If we now consider the time evolution $t_3(.)$: $t \in [t_o, t_f] \mapsto t_3(t)$ of the nonactuated axis t_3 on $S^2 - \{\pm e_3\} = \mathcal{U}$, and an initial feasible extended state (of the dynamics of the satellite and the rotors) we can completely reconstruct the time evolution of the states and outputs (here the control torques).

Proof: From (3), a given time evolution $t_3(.)$ on $\mathcal{U}$, fixes $\Lambda[t_3(.)]$. Moreover, (16) gives $\Omega_3(.)$, and (9) gives $\dot{\lambda}(.)$. Time integrating $\dot{\lambda}(.)$ gives $\lambda(.)$. Then, (2) gives the motion attitude $R(.)$ on $\mathcal{V}$ from which, we find from (7), $\Omega(.)$, and $p(.) = R^T(.)\sigma_o$. Next, from (11b) we deduce $\dot{q}(.)$ and by time integration, we find $q(.)$. Then, (13a) gives $\dot{p}(.)$, which once combined with the time differential of (7), gives the $\dot{\Omega}_\alpha(.)$'s ($\alpha = 1, 2$). Introducing them into (13b) finally gives

$$\tau_1 = -J_{s1}\dot{\Omega}_1 - e_1^T(\Omega \times p), \qquad \tau_2 = -J_{s2}\dot{\Omega}_2 - e_2^T(\Omega \times p) \tag{19}$$

where $J_{s\alpha} = J_\alpha - J_{r\alpha}$. Thus, we can reconstruct the time evolution of all internal and external variables. (It is worth noting that because this reconstruction process requires some time integration, the position of the nonactuated axis on the unit sphere does not define a set of flat outputs.) □

Figure 3 summarizes the string of computations used in the proof above.

IV. Path-Planning Strategy

In this section, we will consider the path planning in a finite time interval $[t_o, t_f]$. This constraint will be removed at the end of this section (see remark 2). As a preliminary remark, let us note that the time evolution of λ from its initial value is completely determined by the dynamic constraint (16) and the kinematics (9), that is, by

$$\dot{\lambda} = A\Big(e_3^T t_3\Big) + \omega_{S^2}(\dot{t}_3) \tag{20}$$

Then, let us consider any initial state $x_o \in \mathcal{A}^\circ$, and final one $x_f \in \mathcal{A}_1$ or $\mathcal{A}_2{}^\circ$, and their corresponding points: $[(t_{3o}, \dot{t}_{3o}), (\lambda_o, \dot{\lambda}_o)]$ and $[(t_{3f}, \dot{t}_{3f}), (\lambda_f, \dot{\lambda}_f)]$ on $T\mathcal{U} \times T\mathrm{SO}(2)$. Because $\dot{t}_{3f} = 0$ for O1 and O2, Eq. (20) forces the relation $\dot{\lambda}_f = A(e_3^T t_{3f})$. Thus, only $(t_{3f}, \dot{t}_{3f}, \lambda_f)$ can be fixed arbitrarily by the path-planning algorithm whereas $\dot{\lambda}_f$ is imposed by the kinetic momentum conservation law. Finally, any desired motion $t_{3d}(.)$ on $\mathcal{U}$, such that: $t_{3d}(t_o) = t_{3o}$, $\dot{t}_{3d}(t_o) = \dot{t}_{3o}$, $t_{3d}(t_f) = t_{3f}$, $\dot{t}_{3d}(t_f) = 0$; solves the path planning for the two objectives if, and only if, it also satisfies

$$\lambda_f - \lambda_o = \Delta\lambda_f = \int_{t_o}^{t_f} A\Big(e_3^T t_{3d}\Big)\, \mathrm{d}t + \int_{t_{3d}(.) \subset \mathcal{U}} \omega_{S^2}(\dot{t}_{3d}) \tag{21}$$

Then, based on assertion 2, the reachability of $\mathcal{A}_1$ and $\mathcal{A}_2{}^\circ$ from $\mathcal{A}^\circ$ is proved.

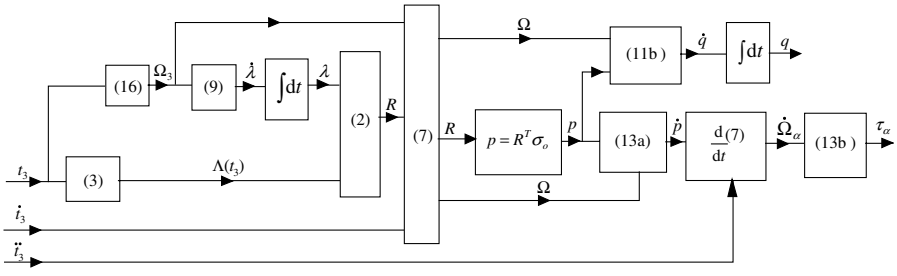

Fig. 3 Block diagram of the open-loop control computation.

Remark 1: Geometric Nature of the Problem: At this point, let us note that when $\sigma_o = 0$ then $A = 0$ in (21) and the existence of feasible paths on $\mathcal{U}$ producing any desired shift $\Delta\lambda_f = \lambda_f - \lambda_o$ in the fiber, is guaranteed by $\mathrm{hol}(S^2) = \mathrm{SO}(2)$, where $\mathrm{hol}(S^2)$ is the holonomy group [16] of S^2, that is, the group of transformations applied to the frame (t_1, t_2) tangent to S^2, and generated by the parallel transport along all the curves of S^2 (c.f. Fig. 2). Finally, the path-planning problem is also related to the "falling cat and gauged theory" [1]. In this theoretical framework when $\sigma_o = 0$, $\Delta\lambda_f$ stands for a "kinematic phase," whereas when $\sigma_o \neq 0$, the first term of (21) adds a "dynamic phase" to the kinematic one. In this last case, the holonomy of S^2 and the context of Fig. 2 are not sufficient for stating the reachability. The purpose of the following sections is to prove the reachability in this more general case.

Remark 2: Asymptotic Control, Definitions of Reachability for O1 and O2: In Secs. V and VI which follow, the state of the unactuated axis $(t_{3d}, \dot{t}_{3d})$ will be planned on an infinite time interval $[t_o, +\infty[$ and the final conditions of the path will be $t_{3d}(+\infty) = t_{3f}$ and $\dot{t}_{3d}(+\infty) = \dot{t}_{3f} = 0$. In these conditions, note that if the kinematic phase [the second term of (21)] converges to a finite value when $t_f \to +\infty$. On the other hand, the dynamic phase

$$J_f = \lim_{t_f \to +\infty} \int_{t_o}^{t_f} A\left(e_3^T t_{3d}\right) \mathrm{d}t$$

converges only if $A = 0$, or $[e_3^T t_{3d}(t_f)] \to 0$, that is, in the case of objective O1 Hence, when planning $(t_{3d}, \dot{t}_{3d})$ on an infinite time interval only, $\mathcal{A}_1$ can be reached asymptotically. This means that for objective O2, the verification of (21) with $t_f \to +\infty$ makes no sense because in this case λ cannot asymptotically converge to λ_f while $\dot{\lambda} \to \dot{\lambda}_f = A(e_3^T t_{3f}) \neq 0$. Hence, in the following, the reachability of $\mathcal{A}_1$ will mean "asymptotic reachability," whereas $\mathcal{A}_2$ will be considered as "reachable" when we are able to find an open-loop control law on $[t_o, t_f] \subset \mathbb{R}^+$ which steers x from any $x_o \in \mathcal{A}$ to any $x(t_f) \in \mathcal{A}$, with t_f sufficiently large to obtain $t_3(t_f) \simeq t_{3f}, \dot{t}_3(t_f) \simeq 0$ whereas $\lambda(t_f) = \lambda_f, x_f = [t_{3f}, 0, \lambda_f, \dot{\lambda}_f = A(e_3^T t_{3f})] \in \mathcal{A}_2$ and "$\simeq$" is an approximation whose accuracy increases with t_f.

V. Restricted Reachability

We will first investigate the (restricted) reachability of $\mathcal{A}_1$, $\mathcal{A}_2{}^\circ$ from $\mathcal{A}^\circ$. It is based on the stereographic projection [14]. The results of reachability in this section will be extended to $\mathcal{A}_2$ and $\mathcal{A}$ in the next section.

A. Stereographic Projection (Fig. 4)

From planar geometric considerations (see Fig. 4), we find, with $P_{e_3}(t_3)$ the projection of t_3 from e_3 in the equatorial plane and $\eta \triangleq [P_{e_3}(t_3)^T P_{e_3}(t_3)]^{1/2} = \|P_{e_3}(t_3)\|$:

$$\cos\psi = (\eta^2 - 1)(\eta^2 + 1)^{-1}, \qquad \sin\psi = 2\eta(\eta^2 + 1)^{-1} \tag{22}$$

Thus, $(\mathcal{U}, \eta, \varphi)$ defines a new chart on S^2, with $\eta \geq 0$, and $\varphi \in \mathbb{R}$.

B. Path-Planning Algorithm

In this subsection t_f can be finite (O2) or infinite (O1) (see remark 2 of Sec. IV). Because (21) is invariant by any rotation around the symmetry axis of poles, we will take as reference variables (from which we can recover all the internal and external variables in the same manner as that of the proof of assertion 2):

$$\eta \quad \text{and} \quad \xi \triangleq \dot{\varphi}/(1 + \eta^2) \tag{23}$$

Hence, with $t \in [t_o, t_f]$, the desired time evolutions $\eta_d(.)$ and $\xi_d(.)$ have to satisfy $\eta_d(.) \geq 0$, and the two following integral conditions, both imposed by the boundary conditions on φ and λ:

$$\varphi_f - \varphi_o = \Delta\varphi_f = \int_{t_o}^{t_f} \left(1 + \eta_d^2\right)\xi_d \, \mathrm{d}t \tag{24a}$$

$$\lambda_f - \lambda_o = \Delta\lambda_f = \int_{t_o}^{t_f} \left[A\left(1 + \eta_d^2\right)^{-1} - \xi_d\right]\left(\eta_d^2 - 1\right) \mathrm{d}t = J_f - \int_{t_o}^{t_f} \xi_d\left(\eta_d^2 - 1\right) \mathrm{d}t \tag{24b}$$

where the first integral is the result of replacing φ by ξ, whereas the second is a parametrization of (21) by (23) with J_f the "dynamic phase."

Finally we will also impose $\eta_d(.)$ and $\xi_d(.)$ to verify the following initial conditions:

$$\eta_d(t_o) = \eta_o, \qquad \dot{\eta}_d(t_o) = \dot{\eta}_o, \qquad \xi_d(t_o) = \xi_o = \dot{\varphi}_o/\eta_o \tag{25}$$

whereas, in accordance to the remark 2 of Sec. IV, the following final conditions must be imposed:

for O1:

$$\eta_d(+\infty) = \eta_f, \qquad \dot{\eta}_d(+\infty) = 0, \qquad \xi_d(+\infty) = 0 \tag{26}$$

and $t_f = +\infty$ in (24),

for O2:

$$\eta_d(t_f) \simeq \eta_f, \qquad \dot{\eta}_d(t_f) \simeq 0, \qquad \xi_d(t_f) \simeq 0 \tag{27}$$

and t_f is finite in (24).

Finally η_o and η_f are strictly positive and bounded, because: t_{3o}, $t_{3f} \in \mathcal{U}$. Then, we have the following assertion.

Assertion 3: Reachability of $\mathcal{A}_1$ and $\mathcal{A}_2{}^\circ$ from $\mathcal{A}^\circ$: With the following time evolution for (23):

$$\eta_d(t) = a_o + \sum_{i=1}^{2} a_i e^{-\lambda_i t} \tag{28a}$$

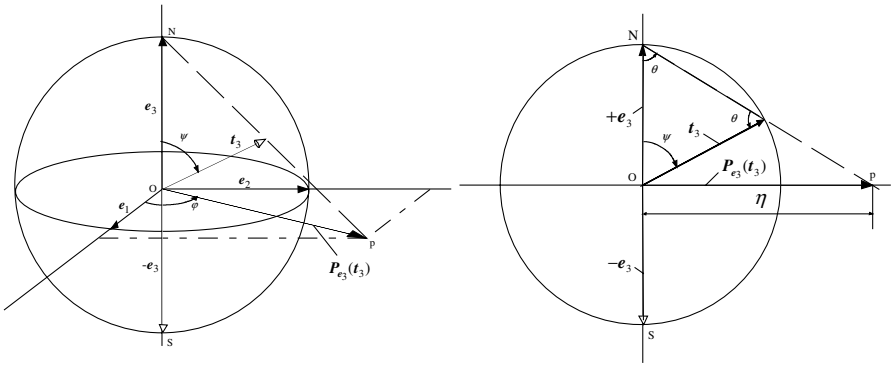

Fig. 4 Stereographic projection.

$$\xi_d(t) = \sum_{j=1}^{3} b_j e^{-\beta_j t} \tag{28b}$$

Two sets of bounded real parameters $(a_i, \lambda_i)_{i=o,1,2}$ and $(b_j, \beta_j)_{j=1,2,3}$ can always be found (with the λ_i's and β_j's positive and distinct), such that (24–27) are verified under the constraint: $\eta_d > 0$. Hence, from assertion 2, $\mathcal{A}_1$ and $\mathcal{A}_2{}^\circ$ are reachable (in the sense of the remark 2 of IV) from $\mathcal{A}^\circ$.

Remarks about (28): The choice of (28) and (23) is justified by the fact that in this case the analytic "by quadrature integration" of (24) is possible. Furthermore, (28) is invariant with respect to the initial time t_o and so enabling us to impose $t_o = 0$ in all subsequent developments. Finally, (28) is such that the accelerations (and so the control torques) tend asymptotically to zero on the target.

Proof of Assertion 3: It is necessary to use the following lemma to guarantee the constraint: $\eta_d > 0$ on $\mathcal{U} = S^2 - \{\pm e_3\}$.

Lemma (Proved in the Appendix): For any initial conditions $\eta_o \geq 0$ and $\dot{\eta}_o$ (with $\dot{\eta}_o > 0$, if: $\eta_o = 0$, and $\dot{\eta}_o \in \mathbb{R}$, in any other case), and for any desired final value $\eta_f \geq 0$, there always exist sufficiently high λ_1 and λ_2 so that the trajectory $\eta_d(.)$ defined by (25) and (26) and (28a), is such that $\eta_d(t) > 0$ for all $t \in]0, +\infty[$. Moreover, if $\eta_o > 0$, there exist λ_1 and λ_2 such that $\eta_d(t) > 0$ for all $t \in [0, +\infty[$.

For both objectives we consider (28) with the boundary conditions (25) and (26) which impose to the a_i's to satisfy " $a_o = \eta_f$," and the following linear system:

$$\begin{pmatrix} 1 & 1 \\ -\lambda_1 & -\lambda_2 \end{pmatrix} \begin{pmatrix} a_1 \\ a_2 \end{pmatrix} = \begin{pmatrix} \eta_o - \eta_f \\ \dot{\eta}_o \end{pmatrix} \tag{29}$$

where because λ_1 and λ_2 are distinct, (29) is always invertible. Moreover, from the lemma there always exist λ_1 and λ_2 such that: $\eta_d(t) > 0$, $\forall\ t \in [0, +\infty[$. Once (29) solved and $\eta_d(.)$ known, we calculate (this is achieved numerically in the algorithm) the dynamic phase J_f of (24b) on $[0, t_f]$ for O2 and $[0, +\infty[$, for O1 (see remark 2 of IV). Then, (24–26) impose to the b_i's, to verify the following linear system:

$$\begin{pmatrix} 1 & 1 & 1 \\ 1/\beta_1 & 1/\beta_2 & 1/\beta_3 \\ B_{31} & B_{32} & B_{33} \end{pmatrix} \begin{pmatrix} b_1 \\ b_2 \\ b_3 \end{pmatrix} = \begin{pmatrix} \xi_o \\ (1/2)(\Delta\lambda_f + \Delta\varphi_f - J_f) \\ \Delta\varphi_f - \left[\left(1 + \eta_f^2\right)/2\right](\Delta\lambda_f + \Delta\varphi_f - J_f) \end{pmatrix} \tag{30}$$

with $B_{3j} = 2\eta_f \sum_{i=1}^{2} a_i[1/(\lambda_i + \beta_j)] + \sum_{i,k=1}^{2} a_i a_k[1/(\lambda_i + \lambda_k + \beta_j)]$. Because the λ_i's and the β_i's are distinct and arbitrary, (30) is singular only when $a_1 = a_2 = 0$. This corresponds to a "path singularity" that will be dealt with in Sec. VI.A. Moreover, once (29) and (30) are solved, we deduce $\varphi_d(.)$ and $\lambda_d(.)$ from (24) with t now replacing t_f. Then, from (4), we find $t_{3d}(.)$. Thus, in the case of O1, using assertion 2, we can reconstruct the desired control torques (19) on $[0, +\infty[$, which asymptotically steer the spacecraft from any state of $\mathcal{A}^\circ$ to any one of $\mathcal{A}_1$. Finally, as far as O2 is concerned, the same reconstruction works on $[0, t_f]$, and we can always choose t_f such that (27) is satisfied with $\lambda(t_f) = \lambda_f$. □

VI. Global Reachability

To extend the reachability of $\mathcal{A}_2$ and $\mathcal{A}$ to the whole unit sphere, we have to deal with the singularities of the parametrization (η, ξ) on the unit sphere. We will start by the "path singularities" mentioned above and we will later investigate the case of the polar singularities of the unit sphere.

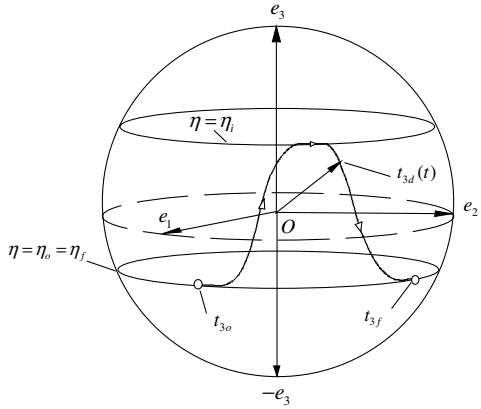

Fig. 5 Escaping from "path singularity".

A. Path Singularities

As mentioned earlier, with $\eta_o = \eta_f$, and $\dot{\eta}_o = 0$, (29) imposes $a_1 = a_2 = 0$, and so making (30) singular. To circumvent this path singularity, we take a piecewise continuous time evolution $\eta_d(.)$ defined as follows (where $t_i \in]0, +t_f[$ is an "intermediate time"):

1°) If: $t < t_i$: $\eta_d(.)$ is given by (28) and (29) with $\eta_f = \eta_i$.

2°) If: $t \geq t_i$: $\eta_d(.)$ is given by (28) and (29) with $(\eta_o, \dot{\eta}_o) = (\eta_i, 0)$ and $t - t_i$ replacing t.

Where " $\eta = \eta_i (\neq \eta_o = \eta_f)$" is an intermediate circle of the sphere on which t_3 transits, and for any $\varepsilon > 0$, the intermediate time: $t_i = t_i(\varepsilon)$ is such that: $\sup(|\eta_d(t) - \eta_i|, |\dot{\eta}_d(t)|) \leq \varepsilon$, $\forall\ t \geq t_i$. Finally, $\xi_d(.)$ remains given by (28b), with the b_i's fixed by (30) where J_f is now piecewising computed, and ξ_o, $\Delta\varphi_f$, and $\Delta\lambda_f$ are fixed without considering the transition. This principle is illustrated in Fig. 5.

B. Polar Singularities

The purpose of the following is to extend the reachability results of Sec. V from sets $\mathcal{A}^\circ$, $\mathcal{A}_2{}^\circ$ to $\mathcal{A}$ and $\mathcal{A}_2$.

1. *Continuous Prolongation of the Path-Planning to the South Pole*

On the north pole ($t_3 = +e_3$): $\eta = +\infty$, and so making any path (28) starting or arriving at $+e_3$ unfeasible. However, on $-e_3$:

$$\begin{aligned} &\eta = 0, \qquad \dot{\eta} = (1/2)\|\dot{t}_3\| = (1/2)\sqrt{\Omega_1^2 + \Omega_2^2} \geq 0 \\ &\varphi - \lambda = \arctan\left[\left(e_2^T t_1\right), \left(e_1^T t_1\right)\right], \qquad \dot{\lambda} - \xi = \Omega_3 \end{aligned} \tag{31}$$

And so (28–30) can be continuously prolonged to $-e_3$ as starting point, with initial conditions:

$$\begin{aligned} &\eta_o = 0, \qquad \dot{\eta}_o = (1/2)\sqrt{\Omega_{1o}^2 + \Omega_{2o}^2}, \qquad \xi_o = 0 \\ &\varphi_o = 0, \qquad \lambda_o = -\arctan\left[\left(e_2^T t_{1o}\right), \left(e_1^T t_{1o}\right)\right] \end{aligned} \tag{32}$$

Moreover, fixing the final conditions:

$$\begin{aligned} &\eta_f = 0, \qquad \xi_f = 0, \qquad \varphi_f = 0 \\ &\lambda_f = -\arctan\left[\left(e_2^T t_{1f}\right), \left(e_1^T t_{1f}\right)\right] \end{aligned} \tag{33}$$

also prolongs (28–30) to $-e_3$ as arrival point. Finally, from the lemma, such a continuous prolongation is always possible with $\eta_d(t) \geq 0$, $\forall\ t \in [0, +\infty[$.

2. *Antipodal Stereographic Projection*

To circumvent the north pole singularity ($+e_3$), let us introduce $P_{-e_3}(.)$, the stereographic projection from the south pole ($-e_3$). It defines a new coordinate η_- (instead of $\eta_+ \triangleq \eta$) related to the angle: $\psi_- = \pi - \psi_+$ (where: $\psi_+ \triangleq \psi$), as η_+ is related to ψ_+. Hence,

inserting $\psi_+ = \pi - \psi_-$ into (2) and (3), with ψ_- defined by $\cos\psi_- = (\eta_-^2 - 1)(\eta_-^2 + 1)^{-1}$ and $\sin\psi_- = 2\eta_-(\eta_-^2 + 1)^{-1}$, gives us a new parametrization of the satellite's attitude R. Moreover, this parametrization is now defined at $+e_3$ and singular at $-e_3$.

C. Global Path-Planning: Reachability of $\mathcal{A}_1$ and $\mathcal{A}_2$ from $\mathcal{A}$

We are now going to prove the following theorem. It is based on the previous continuous prolongation, and the two stereographic projections with their set of reference variables: $(\eta_+, \xi_+ = \dot\varphi/\eta_+)$ and $(\eta_-, \xi_- = \dot\varphi/\eta_-)$.

Assertion 4: A time evolution (28) or one of its piecewise combinations VI.A applied to (η_+, ξ_+) or (and) (η_-, ξ_-) can always be found and steer the satellite from any x_o of $\mathcal{A}$ to any x_f of $\mathcal{A}_1$ or $\mathcal{A}_2$.

Proof: Let us first introduce the four following state spaces: $\mathcal{A}_\pm \triangleq TW_\pm \cap \mathcal{A}$ and $\mathcal{A}_{2\pm} \triangleq TW_\pm \cap \mathcal{A}_2$. Hence, $\mathcal{A}_\pm$ (respectively, $\mathcal{A}_{2\pm}$) are the two subspaces of $\mathcal{A}$ (respectively, of $\mathcal{A}_2$), such that $R(\pm e_3) = \pm e_3$. Therefore, because of assertion 3, and $\mathcal{A} = \mathcal{A}^\circ \cup \mathcal{A}_+ \cup \mathcal{A}_-$, $\mathcal{A}_2 = \mathcal{A}_2{}^\circ \cup \mathcal{A}_{2+} \cup \mathcal{A}_{2-}$, assertion 4 is proved by the fact that

1°) $\mathcal{A}_1$ and $\mathcal{A}_2{}^\circ$ are reachable from $\mathcal{A}_-$ (respectively, $\mathcal{A}_+$), by applying the path (28) with the initial conditions (32) to (η_+, ξ_+) [respectively, to (η_-, ξ_-)].

2°) $\mathcal{A}_{2-}$ (respectively, $\mathcal{A}_{2+}$) is reachable from $\mathcal{A}^\circ$, by applying (28) with the final conditions (33) to (η_+, ξ_+) [respectively, to (η_-, ξ_-)].

3°) $\mathcal{A}_{2+}$ and $\mathcal{A}_{2-}$ are reachable from $\mathcal{A}_+$ and $\mathcal{A}_-$, that is (24b) can be satisfied while steering t_3: a) from one pole back to itself, and, b) from one pole to the other.

3a) In the first subcase a), if the pole is the south pole (and, respectively, the north pole) apply (28), with initial and final conditions (32) and (33) to (η_+, ξ_+) [respectively, to (η_-, ξ_-)]. From (32) and (33), one path singularity occurs. To escape from this, the piecewise combination of Sec. VI.A must be used (see Fig. 6a).

3b) In the second subcase b), if starting from the south pole (respectively, the north one) apply (28) with (32) to (η_+, ξ_+) [respectively, to (η_-, ξ_-)] and then transit on the equator by imposing $\eta_{+i} = 1$ (respectively, $\eta_{-i} = 1$) in the piecewise combination of Sec. VI.A. While transiting on the equator, use the equatorial symmetry property: $\eta_{+i} = \eta_{-i} = 1$; to change η_+ into η_- (respectively, η_- into η_+), and steer the satellite to the north pole (respectively, the south) with η_- (respectively, η_+) fixed by (33), and initial regular conditions fixed by the transition (see Fig. 6b). □

VII. Simulation Results

All the numerical examples are based on the following data:

$$(J_{s1}, J_{s2}, J_{s3}) = (300, 200, 290)\ \text{kg.m}^2, \qquad J_{r1} = J_{r2} = 10\ \text{kg.m}^2$$

The satellite's dynamics are numerically time integrated using quaternions. We will now report two simulation results of the control law (19) with the previous path planning. The first test deals with the control objective O1, the second with O2. The first test concerns a regular case whereas the second corresponds to the most perverse case when going from one pole to the other.

Test 1: O1, regular case (Fig. 7): The conditions of the test are the following: $t_f = 1500$, $\beta_1 = 10\beta_2 = 100\beta_3 = 5\lambda_1 = 50\lambda_2 = 0.5$, $\psi_o = 3\pi/4$, $\psi_f = 2\varphi_o = 2\lambda_o = \pi/2$, $\varphi_f = \lambda_f = 0$, $\dot q_{1o} = -\dot q_{2o} = 10$, and $\sigma_o = 0.6e_3$.

Test 2: O2, singular case (Fig. 8): For this test: $t_f = 1.10^4$, $t_i = t_f/2$, $\beta_1 = 10\beta_2 = 100\beta_3 = \lambda_1 = 10\lambda_2 = 0.1$, $\psi_o = \pi$, $\lambda_o = 3\pi/2$, $\varphi_o = \psi_f = \varphi_f = \lambda_f = 0$, $\dot q_{o1} = 0$, $\dot q_{o2} = 12$, $\sigma_o = 0.6e_3$.

C. Comments on the Results

As far as test 1 is concerned, when t_3 is steered to the equatorial plane, the kinetic momentum is totally (asymptotically) transferred from the spacecraft to the wheels and the attitude state converges to a feasible rest state. In test 2, the kinetic momentum is transferred to the rotation about the unactuated spacecraft axis. This appears in Fig. 8, where if Ω_1 and Ω_2 both converge asymptotically to zero, this is not the case of Ω_3 which tends to $\dot\lambda_f = A(e_3^T t_{3f}) \simeq 0.0021$ rad/s. Finally, let us point out that for test 1, $\lim_{t\to+\infty}\lambda = \lambda_f$, whereas for test 2, $\lambda(t_f) = \lambda_f$. Hence, five attitude state variables are controlled.

VIII. Conclusions

The article proposes some constructive and explicit solutions to the open-loop control problem of steering the attitude of a two-wheeled satellite from any feasible state to two sets of objectives compatible with the momentum conservation and one rotor failure. For these two objectives, the path planning is based on the same strategy. First, the time evolution of two reference variables describing the motion of the nonactuated axis on the unit sphere are fixed to verify some boundary conditions and the conservation of the angular momentum. Second, all the internal and control variables are recovered from these two variables. Geometrically, it is the curvature of the unit sphere that allows us to recover the lost actuated degree of freedom. The reference variables are deduced from two antipodal stereographic projections and reduced on a truncated basis of exponentials whose the basis parameters are computed explicitly. Finally, the open-loop control proposed here will be used later to achieve a nonsmooth feedback law based on a receding horizon strategy. Then, on the basis of this feedback control law, the problem of robustness will be tackled. Concerning this point, let us note that the satellite with two wheels does not pose the robustness problem in a standard manner. The errors on inertia parameters or the presence of external perturbing torques modifies the angular momentum conservation law, and consequently, the reachable control objectives.

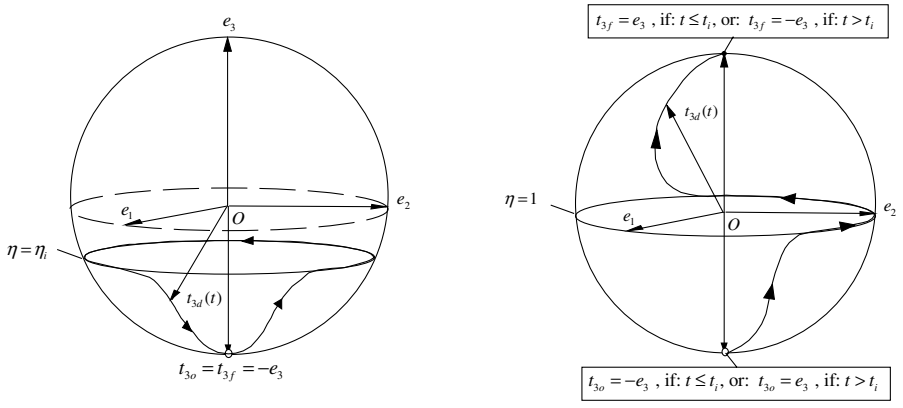

a) **b)**

Fig. 6 Going from one pole back to itself and to the other (cases 3a and 3b of control objective O2).

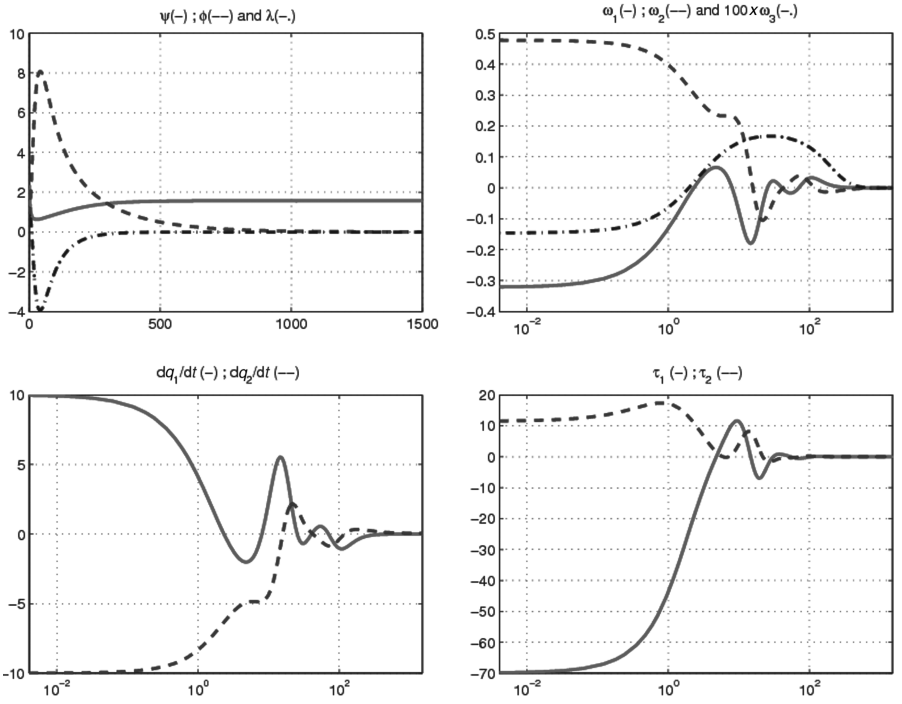

Fig. 7 O1 in the regular case.

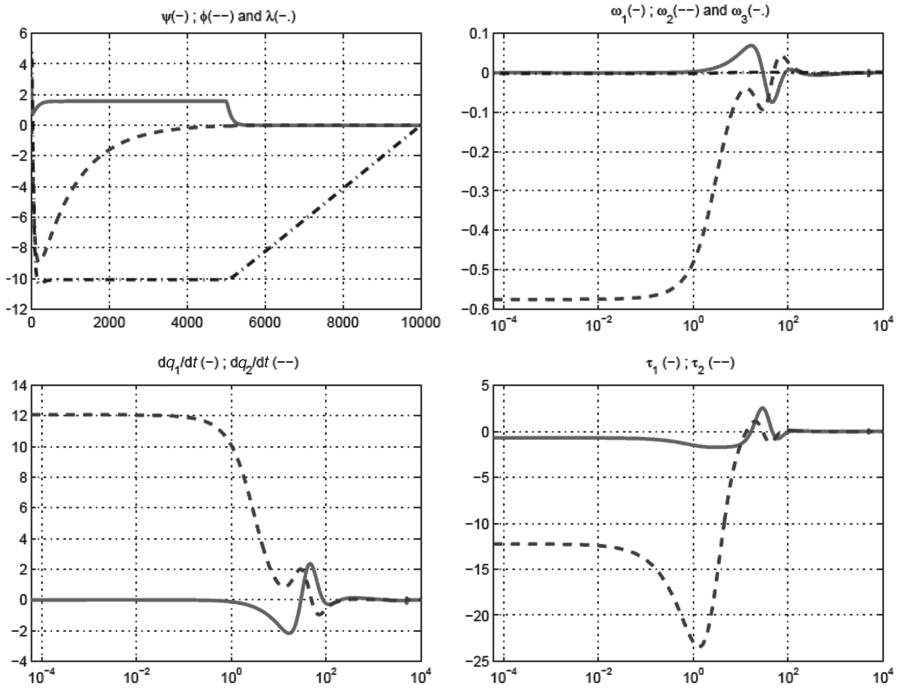

Fig. 8 O2 in the singular case.

Appendix

Proof of lemma of Sec. V: Then simple computation leads to the following expression of $e(t) = \eta(t) - \eta_f$ in the case where $\lambda_1 = (1/2)\lambda_2 = \lambda$:

$$e(t) = a(t)e(0) + (1/\lambda)(a(t) - e^{-\lambda t})\dot{\eta}(0) \tag{A1}$$

where $a(t) = 2e^{-\lambda t} - e^{-2\lambda t}$ which is a strictly decreasing positive function that is <1 for all $t > 0$. Therefore, all we have to prove is that $e(t) > -\eta_f$ for all $t > 0$. Two situations have to be distinguished: 1) if $\dot{\eta}(0) \geq 0$ then $e(t) \geq a(t)e(0)$ which meets the required condition given the property of $a(t)$. 2) If $\dot{\eta}(0) < 0$, then one necessarily has $\eta(0) > 0$ (one cannot go beyond the north pole) and hence $e(0) = \delta - \eta_f$ for some $\delta > 0$. Taking $\lambda > 0$ sufficiently high to have $(1/\lambda)|\dot{\eta}(0)| < \delta/2$, Eq. (A1) writes

$$e(t) \geq a(t)(\delta/2 - \eta_f) + (\delta/2)e^{-\lambda t} \tag{A2}$$

which is greater than $-\eta_f$ for all t. □

References

[1] Montgomery, R., "Gauge Theory and the Falling Cat," in *Dynamics and Control of Mechanical Systems: The Falling Cat and Related Problems*, edited by Michael J. Enos, American Mathematical Society, Providence, R.I., 1992.

[2] Bonnard, B., "Controllabilité des Systèmes Mécaniques sur les

Groupes de Lie," *SIAM Journal on Control and Optimization*, Vol. 22, No. 5, 1984, pp. 711–722.

[3] Crouch, P. E., "Spacecraft Attitude Control and Stabilization: Applications of Geometric Control Theory to Rigid Body Models," *IEEE Transactions on Automatic Control*, Vol. 29, No. 4, 1984, pp. 321–331.

[4] Morin, P., Samson, C., Pomet, J. B., and Jiang, Z. P., "Time Varying Feedback Stabilization of a Rigid Spacecraft with Two Controls," *Systems and Control Letters*, Vol. 25, No. 5, 1995, pp. 375–385.

[5] Coron, J. M., and Kerai, E. Y., "Explicit Feedbacks Stabilizing the Attitude of a Rigid Spacecraft with Two Control Torques," *Automatica*, Vol. 32, No. 5, 1996, pp. 669–677.

[6] Alamir, M., and Boyer, F., "Fast Generation of Attractive Trajectories for an underactuated Satellite, Application to Feedback Control Design" *Optimization and Engineering*, Vol. 4, 2003, pp. 215–230.

[7] Tsiotras, P., and Doumtchenko, V., "Control of Spacecraft Subject to Actuator Failures: State-of-the-Art and Open Problems," *Journal of the Astronautical Sciences*, Vol. 48, Nos. 2 and 3, 2000, pp. 337–358.

[8] Krishnan, H., Mc Clamroch, N. H., and Reyhanoglu, M., "Attitude Stabilization of a Rigid Spacecraft Using Two Momentum Wheel Actuators," *Journal of Guidance, Control, and Dynamics*, Vol. 18, No. 2, 1995, pp. 256–263.

[9] Horri, N. M., and Hodgart, S., "Attitude Stabilization of an Underactuated Satellite Using Two Wheels," *Proceedings of the IEEEAC Conference*, Vol. 6, 2002, pp. 2629–2635.

[10] Kim, S., and Kim, Y., "Spin Axis Stabilization of a Rigid Spacecraft Using Two Reaction Wheels," *Journal of Guidance, Control, and Dynamics*, Vol. 24, No. 5, 2001, pp. 1046–1049.

[11] Fliess, M., Lévine, J., Martin, Ph., and Rouchon, P., "Flatness and Defect of Nonlinear Systems: Introductory Theory and Examples," *International Journal of Control*, Vol. 44, No. 5, 1999, pp. 922–937.

[12] Alamir, A., and Marchand, N., "Numerical Stabilisation of Non-Linear Systems: Exact Theory and Approximate Numerical Implementation," *European Journal of Control*, Vol. 5, 1999, pp. 87–97.

[13] Tsiotras, P., and Longuski, J. M., "Spin-Axis Stabilization of Symmetric Spacecraft with Two Control Torques," *Systems and Control Letters*, Vol. 23, 1994, pp. 395–402.

[14] Tsiotras, P., and Longuski, J. M., "A New Parameterization of the Attitude Kinematics," *Journal of the Astronautical Sciences*, Vol. 43, No. 3, 1995, pp. 243–262.

[15] Tsiotras, P., Corless, M., and Longuski, J. M., "A Novel Approach to the Attitude Control of an Axisymmetric Spacecraft," *Automatica*, Vol. 31, No. 8, 1995, pp. 1099–1112.

[16] Petersen, P., "Symmetric Spaces and Holonomy," *Riemannian Geometry, Graduate Texts in Mathematics*, Springer, New York, 1998, pp. 205–242.